

Microscale Patterning of Hydrophobic/Hydrophilic Surfaces by Spatially Controlled Galvanic Displacement Reactions

L. Rizzello,[†] S. Shiv Shankar,[†] D. Fragouli, A. Athanassiou, R. Cingolani, and P. P. Pompa*

National Nanotechnology Laboratory of CNR-INFM, IIT Research Unit, Via per Arnesano, 73100 Lecce, Italy.

[†] Equally contributing authors

Received March 13, 2009. Revised Manuscript Received April 8, 2009

In this letter, we report the design and fabrication of different metal patterns for the realization of spatially controlled hydrophobic/hydrophilic regions with micrometer resolution. The fabrication procedure, based on a combination of lithographic techniques and wet-chemistry reactions (namely, spontaneous Galvanic displacement reactions) is reliable, undemanding, and highly versatile, allowing the achievement of precise spatial control along with the use of a wide variety of different materials.

Introduction

The spatial control of hydrophobic/hydrophilic surfaces is a key target of considerable research because of its importance in many technological fields, including MEMS devices,¹ epithelial cell adhesion,² separation of different chemical environments,³ creation of transparent glasslike films with self-cleaning effects,⁴ patterning of biomolecules or nanoparticles,^{5,6} and development of microfluidic channels or laboratory-on-a-chip systems.^{7,8} Superhydrophobicity, though being of interest for current advanced materials, is a well-known natural strategy. *Nelumbo nucifera* (lotus) plant leaves exhibit, for instance, superhydrophobic behavior thanks to their combined micro- and nanostructured surface architecture so that dirt particles can be picked up by rolling water droplets (self-cleaning effect);⁹ moreover, water strider legs¹⁰ and cicada wings¹¹ have particular nanoscale features that allow these insects to stand and/or walk over water surfaces. This special behavior of superhydrophobicity, typically achieved on specially designed or naturally occurring nanostructured surfaces, is generally referred to as the lotus effect.¹² Because water's interactions with solids are limited to their outer layers, it is possible in principle to imitate and reproduce such lotus effect by properly engineering the morphological properties of

particular surfaces.^{13–15} For this reason, many methods, including chemical or plasma etching,^{16,17} optical and e-beam lithography,^{18–20} sol–gel methods,¹ electrochemistry,^{21–23} laser ablation,²⁴ and galvanic displacement reactions,^{13,25} have been applied to make surfaces superhydrophobic by controlling their surface patterns. However, although these strategies are well established, there are only few reports so far in which precise spatial control of hydrophobic/hydrophilic regions has been demonstrated. For instance, Zhang and co-workers¹⁶ have recently reported an easy and elegant method of patterning hydrophilic–hydrophobic stripes over TiO₂ surfaces by the selective photocatalytic decomposition of octadecylphosphonic acid (ODP) monolayers via UV irradiation. Such a technique, however, is not very versatile because it cannot allow the fabrication of such patterns over different substrates and the realization of submicrometer features due to the resolution limit of photolithography. In this letter, spontaneous galvanic displacement reactions (SGDR) have been exploited to roughen flat silver (Ag) or silicon (Si) substrates to create nanostructured gold films. Using the SGDR-based technique, we were able to fabricate nanorough metallic substrates with efficient hydrophobic or hydrophilic properties conveniently, depending on the surface chemistry modification. Furthermore, by combining such a chemical approach with well-established lithographic techniques, we were able to fabricate metal patterns with different surface morphologies. This ensures precise spatial control of hydrophobic/hydrophilic regions on a wealth of substrates. In principle, by integrating this strategy with e-beam lithography, it is possible to

*Corresponding author. Tel: +39-0832-295714. Fax: +39-0832-298180. E-mail: piero.pompa@unile.it.

- (1) Xiu, Y.; Zhu, L.; Hess, D. W.; Wong, C. P. *Proc. HDP'07* **2007**, 1–5.
- (2) Dewez, J. L.; Schneider, Y. J.; Rouxhet, P. G. *J. Biomed. Mater. Res.* **1996**, *30*, 373–383.
- (3) Feng, L.; Zhang, Z.; Mai, Z.; Ma, Y.; Liu, B.; Jiang, L.; Zhu, D. *Angew. Chem., Int. Ed.* **2004**, *43*, 2012–2014.
- (4) Bravo, J.; Zhai, L.; Wu, Z.; Cohen, R. E.; Rubner, M. F. *Langmuir* **2007**, *23*, 7293–7298.
- (5) Shiu, J. Y.; Chen, P. *Adv. Funct. Mater.* **2007**, *17*, 2680–2686.
- (6) Piret, G.; Coffinier, Y.; Roux, C.; Melnyk, O.; Boukherroub, R. *Langmuir* **2008**, *24*, 1670–1672.
- (7) Fang, G.; Li, W.; Wang, X.; Qiao, G. *Langmuir* **2008**, *24*, 11651–11660.
- (8) Londe, G.; Chunder, A.; Wesser, A.; Zhai, L.; Cho, H. J. *Sens. Actuators, B* **2008**, *132*, 431–438.
- (9) Sun, T.; Feng, L.; Gao, X.; Jiang, L. *Acc. Chem. Res.* **2005**, *38*, 644–652.
- (10) Gao, X. F.; Jiang, L. *Nature (London)* **2004**, *432*, 36. Gao, X. F.; Jiang, L. *Acc. Chem. Res.* **2005**, *38*, 644–652.
- (11) Lee, W.; Jin, M. K.; Yoo, W. C.; Lee, J. K. *Langmuir* **2004**, *20*, 7665–7669.
- (12) Barthlott, W.; Neinhuis, C. *Planta* **1997**, *1*, 202.
- (13) Safaee, A.; Sarkar, D. K.; Farzaneh, M. *Appl. Surf. Sci.* **2008**, *254*, 2493–2498.
- (14) Roach, P.; Shirtcliffe, N. J.; Newton, M. I. *Soft Matter* **2008**, *4*, 224–240.
- (15) Li, X.-M.; Reinhoudt, D.; Crego-Calama, M. *Chem. Soc. Rev.* **2007**, *36*, 1350–1368.

- (16) Zhang, X.; Jin, M.; Liu, Z.; Tryk, D. A.; Nishimoto, S.; Murakami, T.; Fujishima, A. *J. Phys. Chem. C* **2007**, *111*, 14521–14529.
- (17) Chang, Y. C.; Mei, G. H.; Chang, T. W.; Wang, T. J.; Lin, D. Z.; Lee, C. K. *Nanotechnology* **2007**, *18*, 1–6.
- (18) Huang, X. J.; Lee, J. H.; Lee, J. W.; Yoon, J. B.; Choi, Y. K. *Small* **2008**, *4*, 211–216.
- (19) Kim, T.; Baek, C. H.; Suh, K. Y.; Seo, S. M.; Lee, H. H. *Small* **2008**, *4*, 182–185.
- (20) Martines, E.; Seunarine, K.; Morgan, H.; Gadegaard, N.; Wilkinson, C. D. W.; Riehle, M. O. *Nano Lett.* **2005**, *5*, 2097–2103.
- (21) Wang, M. F.; Raghunathan, N.; Ziaie, B. *Langmuir* **2007**, *23*, 2300–2303.
- (22) Bok, H. M.; Shin, T. Y.; Park, S. *Chem. Mater.* **2008**, *20*, 2247–2251.
- (23) Xu, L.; Chen, W.; Mulchandani, A.; Yan, Y. *Angew. Chem., Int. Ed.* **2005**, *44*, 6009–6012.
- (24) Zorba, V.; Persano, L.; Pisignano, D.; Athanassiou, A.; Stratakis, E.; Cingolani, R.; Tzanetakis, P.; Fotakis, C. *Nanotechnology* **2006**, *17*, 3234–3238.
- (25) Cao, Z.; Xiao, D.; Kang, L.; Wang, Z.; Zhang, S.; Ma, Y.; Fu, H.; Yao, J. *Chem. Commun.* **2008**, *23*, 2692–2694.

achieve nanometer-scale resolution of the patterns, a feature that can be important for some specific applications.

Results and Discussion

In an SGDR process, metal deposition is carried out in the absence of an external reducing agent.^{26–28} The crucial aspect, in this method, is that the standard reduction potential of the sacrificial metal layer should be lower than that of the replacing metal that is intended to be deposited from solution. The deposition reaction proceeds as long as reducing ions in solution are able to permeate into the sacrificial template, displacing it, until such reducing ions are consumed by the reaction or until a dielectric layer of oxidized substrate forms, thereby halting electron transfer. The mechanism of structural evolution during metal deposition by the galvanic displacement reaction has been addressed by some groups in the recent past,²⁸ and mixed potential theories provide a useful tool for predicting the reactivity of a replacing/sacrificial metal pair.²⁹ SGDR techniques have attracted great interest because of their simplicity of operation, cost effectiveness, high throughput, and lack of elaborate equipment,³⁰ so this redox potential-based metal coating is routinely used for several commercial plating processes, usually termed electroless plating.

In our experiments, we initially investigated, by holographic microscopy and atomic force microscopy (AFM), the SGDR reaction over a thin silver film deposited onto a glass substrate to monitor the displacement of the silver layer by gold ions, leading to the formation of a rough gold film. For these experiments, we first deposited by thermal evaporation an Ag film onto an aminopropyltriethoxysilane (APTES)-modified glass slide. The reaction was then carried out by adding H₂AuCl₄ aqueous solution, resulting in the deposition of reduced gold species in their metallic form replacing the oxidized products, Ag⁺ ions. We attempted different reaction conditions by modifying the H₂AuCl₄ concentration and incubation time, as well as Ag thickness and deposition conditions, until we achieved the best surface roughness for optimal control of the hydrophobic/hydrophilic behavior (10⁻³ M H₂AuCl₄ incubation for 10 min at room temperature). In Figure 1a,b, representative holographic microscopy images of the substrate before and after the SGDR process are reported (the visualized area is 50 × 50 μm²). The unreacted flat Ag film (just after the injection of the chloroauric acid solution) is shown in Figure 1a, whereas Figure 1b reveals the different morphology of the film after the Galvanic reaction with gold ions is concluded (typically after a few minutes). The reaction was observed to occur by initial nucleation at numerous sites on the surface followed by growth around such nucleated sites until the reaction stops. It is interesting that the metal film appears to be transformed from a uniform, flat surface (silver) to a substantially different film in terms of topography (gold), exhibiting quite uniform roughness. To characterize the surface morphology of the gold layer accurately, we performed AFM analyses. A typical 3D AFM image of the rough gold film is reported in Figure 1c, clearly showing the presence of a

continuous nanoscale roughness over the SGDR film. Representative AFM line profiles (Figure 1d) of the region revealed a homogeneous nanoroughness, with typical 100–150 nm peak-to-valley values (where the surface roughness of the flat silver film was in the ~1 nm range).

The wettability characteristics of the nanorough gold films were found to be largely modifiable by properly changing their surface chemistry and morphological features. In particular, the deposition of small polar molecules, such as cysteine (Cys), onto the optimized nanorough surface resulted in superhydrophilic behavior (Figure 2b), with a water contact angle (WCA) of ~10 ± 2°; on the other hand, the modification of the substrate with long carbon chain molecules, such as octadecylamine (ODA), led to a significant shift to superhydrophobic behavior (Figure 2d), with a WCA value of ~135 ± 2°. In contrast, the deposition of Cys or ODA molecules onto flat gold substrates did not elicit such large variations in wettability, with WCA values ranging approximately from 55 ± 2° to 88 ± 2° for the Cys- and ODA-modified samples, respectively (Figure 2a–c). We optimized this nanostructured substrate by investigating the behavior of a wide range of SGDR substrates with intermediate values of surface roughness, finding that gold substrates with lower surface roughness exhibited less intense hydrophobic (or hydrophilic) character when functionalized with ODA (or Cys) (not shown here). Additional attempts to further increase the surface roughness of the SGDR substrates by means of this simple solution-based procedure, in order to increase further the surface hydrophobicity, resulted in the fabrication of nonuniform substrates with nonreproducible WCA values.

The diverse wetting behavior of the roughened gold substrates, produced using the SGDR reaction, after their chemical modification with Cys and ODA, can be explained and modeled by means of two distinct hypotheses, classically used to describe the wettability of rough surfaces. The first hypothesis belongs to Wenzel, and assumes that any liquid drop that comes in contact with a rough surface penetrates within the features of the surface, wetting it completely. The Wenzel model is described by the following equation³¹

$$\cos \theta_r = r_w \cos \theta \quad (1)$$

where θ_r and θ are the contact angles of a liquid drop on the rough and flat surfaces with the same chemistry, respectively. The factor r_w is called the surface roughness and is defined as the ratio of the actual surface area over the projected surface area of the sample. The roughness r_w is always greater than unity. Equation 1 predicts that the contact angle of a liquid on a rough surface is decreased compared to that on the flat surface ($\theta_r < \theta$) when the latter is hydrophilic ($\theta < 90^\circ$), whereas it is increased ($\theta_r > \theta$) when the flat surface is hydrophobic ($\theta > 90^\circ$). Applying the Wenzel model to the gold surfaces modified with cysteine, where the WCA of the flat surface is $\theta = 55^\circ$ and that of the rough surface is $\theta_r = 10^\circ$, we calculate a surface roughness of $r_w = 1.71$. Using different line profiles taken on the surfaces of the nanorough gold films, as recorded by AFM measurements presented in Figure 1, we performed simple geometrical calculations to estimate the ratio between the actual surface area over the projected surface area of the sample. This calculation estimates the roughness of the gold surface as defined by the Wenzel model, and it gives an average value of $r = 1.20$. The two values of roughness predicted by the Wenzel model and by the geometrical calculation on the surfaces recorded by AFM exhibit a small difference that can be ascribed

(26) Okinaka, Y.; Hoshino, M. *Gold Bull.* **1998**, *31*, 3–13.

(27) Kato, M.; Sato, J.; Otani, H.; Homma, T.; Okinaka, Y.; Yoshioka, O. *J. Electrochem. Soc.* **2002**, *149*, 164–167.

(28) (a) Au, L.; Lu, X.; Xia, Y. *Adv. Mater.* **2008**, *20*, 2517–2522. (b) Bansal, V.; Jani, H.; Plessis, J. D.; Coloe, P. J.; Bhargava, S. K. *Adv. Mater.* **2008**, *20*, 717–723. (c) Liang, H. P.; Zhang, H. M.; Hu, J. S.; Guo, Y. G.; Wan, L. J.; Bai, C. L. *Angew. Chem., Int. Ed.* **2004**, *43*, 1540–1543.

(29) Osaka, T.; Okinaka, Y.; Sasano, J.; Kato, M. *Sci. Tech. Adv. Mater.* **2006**, *7*, 425–437.

(30) Mallory, G. O., Hajdu, J. B., Eds.; *Electroless Plating: Fundamentals and Applications*; American Electroplaters and Surface Finishers Society: Orlando, FL, 1990.

(31) Wenzel, R. N. *Ind. Eng. Chem.* **1936**, *28*, 988–994.

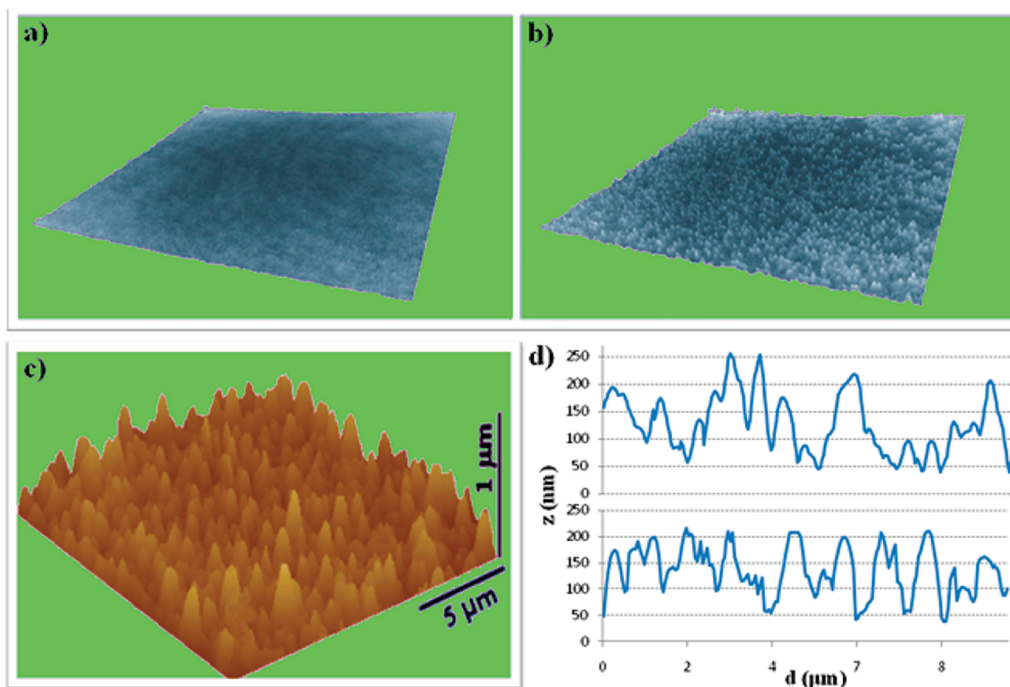


Figure 1. Investigation of an SGDR reaction by holographic microscopy (a, b) and AFM (c, d). A thin silver film, deposited onto an APTES-modified glass coverslip, was displaced by gold (10^{-5} M HAuCl_4 aqueous solution). The surface morphology shifts from a flat silver film (a) before the SGDR reaction to a uniformly nanorough gold surface (b) after the reaction is complete (the visualized region is $50 \times 50 \mu\text{m}^2$). (c) AFM 3D image of the nanorough gold film and (d) two representative line profiles of this region.

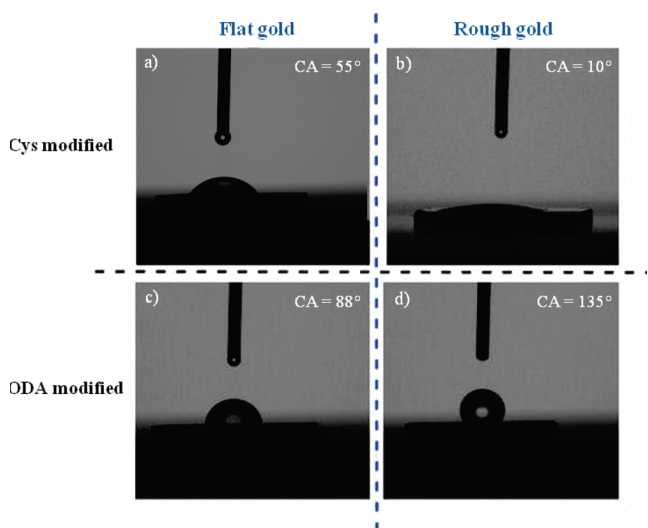


Figure 2. Static water contact angle (WCA) measurements. (a–c) Flat Au film with cysteine and ODA modification, respectively; (b–d) nanorough Au film with cysteine and ODA modification, respectively.

to several parameters, including impurities on the measured surfaces, experimental errors, and so forth.

The Wenzel model cannot be applied in the case of the gold surfaces modified by the ODA molecules because it predicts for this kind of flat surface ($\theta = 88^\circ$) a reduction of the WCA after roughening, which does not correspond to the measured values ($\theta_r = 135^\circ$). Therefore, to describe the wetting behavior of this surface, we used a second classical model, the so-called Cassie–Baxter model, which is the most suitable in our case, as predicted

by the calculations of Lafuma et al.³² According to the Cassie–Baxter hypothesis, capillary effects on the rough surfaces prevent the liquid drops from permeating the roughened structure, allowing air pockets to be trapped underneath the liquid and among the rough features.³³ Therefore, the contact angle of the drop residing on a rough structure, θ_r , is an average between the value in air (180°) and the value on the flat surface (θ) and is given by³³

$$\cos \theta_r = -1 + f(1 + \cos \theta) \quad (2)$$

where f is the solid fraction of the surface in contact with the liquid (f is dimensionless and smaller than unity). The Cassie–Baxter model predicts an enhancement of the hydrophobicity of the rough surface compared to that of the flat surface, independent of the contact angle value (θ) of the latter. This is in agreement with our results on the gold surfaces modified by the ODA molecules. By substituting eq 2 into the WCA on the flat gold surface modified with ODA ($\theta = 88^\circ$) and that on the corresponding rough surface ($\theta_r = 135^\circ$), we can calculate that the water drop sits on a composite surface composed of 28% ODA-modified gold and 71% air (fraction of the rough surface wetted by water is $f = 0.29$).

After the assessment of the efficacy and feasibility of the optimized SGDR process to engineer the surface characteristics in terms of controlled wettability, we demonstrated the possibility to fabricate patterns of flat and nanorough metal regions, thus obtaining patterns of hydrophilic/hydrophobic regions with microscale resolution. We achieved these results by simply combining the SGDR process with standard lithographic techniques. Such substrates were realized by a spatially controlled deposition, through the presence of a specifically patterned resist mask, of thin silver regions (typically ~ 50 nm thick) on a predeposited flat

(32) Lafuma, A.; Quere, D. *Nat. Mater.* **2003**, *2*, 457–460.

(33) Cassie, A. B. D.; Baxter, S. *Trans. Faraday Soc.* **1944**, *40*, 546–551.

gold film, followed by lift-off and SGDR displacement of silver by gold. Obviously, only the silver regions were displaced into rough gold, leading to the fabrication of the desired flat and nanorough patterned gold samples. Representative holographic microscopy and SEM images of such patterned metal substrates with rough gold islands patterns, defined by lithography, over a flat gold film, are shown in Figure 3a,b: rough squares, replacing the sacrificial silver layers, can be clearly observed. The high degree of spatial control of such nanostructured surfaces is evident, even in the case of extended substrates, such as millimeter- or centimeter-sized samples (Figure 3b). To exploit the wide versatility of this approach fully, thus demonstrating its applicability to a variety of substrates, we also fabricated patterns of silicon and gold with different surface morphologies. In the latter case, a resist layer was deposited onto a silicon wafer by spin-coating, and a pattern with micrometer stripes was defined by optical lithography. The Si sample was then immersed in an aqueous solution of chloroauric acid. Because the SGDR process is initiated at the metal surface, only the Si regions exposed to the gold ions solution underwent the displacement reaction, whereas the zones protected by the resist mask remained unreacted. Once the photoresist was removed with acetone, we achieved the desired microscale pattern of adjacent regions of flat Si and rough Au. Also, for these experiments, we optimized the reaction conditions and the incubation time to avoid undesired events, such as the diffusion of gold ions under the resist layer. The final result of this procedure, namely, confined gold stripes with controlled topology onto a flat silicon substrate, is shown in the optical and SEM images reported in Figure 3c,d, respectively. Also, in this case, the reliability and precise spatial control of the process are noticeable.

We then explored such nanostructured patterned samples for the spatial control of hydrophobicity/hydrophilicity. In the case of the Au/Si pattern (Figure 4a), in which the Cys-modified nanorough gold surface was observed to be highly hydrophilic ($\sim 10^\circ$ WCA), we found that the random deposition of small water drops by the needle of a WCA system preferentially resulted in their selective localization onto the rough gold stripes (highlighted by the dashed lines in Figure 4a), whereas the adjacent regions remained dry. Although we tried to force the deposition of the small water drops over the silica area (i.e., in the space between two rough gold stripes), the drops seemed to be much more attracted by the hydrophilic rough gold stripes, leading to the deformation of the drop with a fast shift toward the preferred rough surfaces. Furthermore, in the case of a patterned sample with alternating stripes of flat and Cys-modified nanorough gold, we observed that the deposition of a drop of an aqueous solution of fluorescein on the edge of the sample resulted in clear spatial confinement of the water drop. Representative confocal fluorescence images of the patterned substrate (Figure 4b) revealed that the hydrophilic rough gold stripes guide the flow of FITC solution only above them, thanks to their enhanced hydrophilic behavior ($\sim 10^\circ$) as compared to that of unmodified flat gold ($\sim 81^\circ$). In line with the above results, the fluorescent stripes appear to be clearly confined and well separated from the adjacent flat gold stripes.

In conclusion, we optimized the SGDR process of gold with two model substrates, namely, silver and silicon, producing a controlled, uniform nanorough gold surface. We showed that the nanostructured metal surface may exhibit a conversion from superhydrophilic ($\sim 10^\circ$ WCA) to hydrophobic behavior ($\sim 135^\circ$ WCA) upon modification with Cys and ODA, respectively. Importantly, we demonstrated that, by combining SGDR with lithographic techniques, it is possible to obtain precise patterns with different surface morphologies, and thus wettability properties, by an undemanding, low-cost procedure.

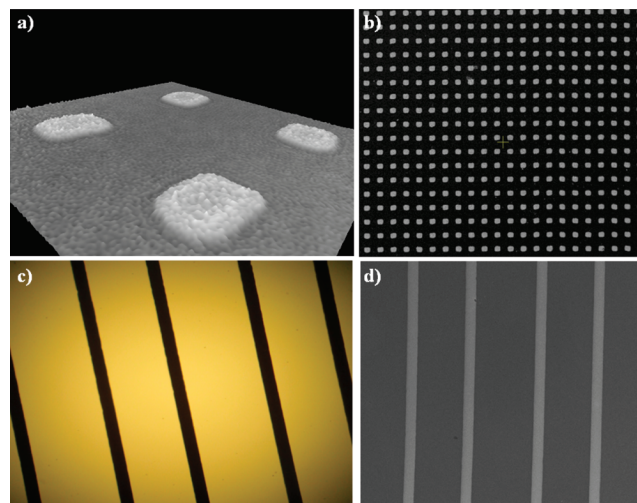


Figure 3. Patterned samples with spatially controlled surface morphology: (top) rough/flat Au; (bottom) rough Au/flat Si. (a) Three-dimensional holographic microscopy image and (b) SEM image of nanorough gold islands ($15 \times 15 \mu\text{m}^2$) on a flat gold film. (c) Optical microscopy image and (d) SEM image of rough gold stripes ($100 \mu\text{m}$ wide) on a Si substrate.

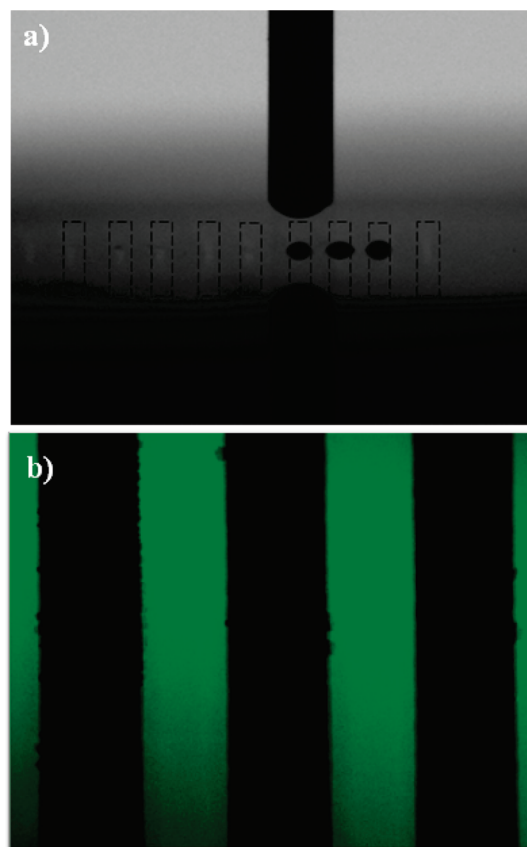


Figure 4. (a) Optical image of small water drops over a pattern of rough gold stripes ($100 \mu\text{m}$ wide) on a Si substrate: the water drops are selectively attracted by the rough hydrophilic stripes, highlighted by the black dashed lines. (b) Confocal image of an FITC aqueous solution over $100\text{-}\mu\text{m}$ -wide rough gold stripes on a flat Au film: the solution is preferentially guided onto the nanorough hydrophilic stripes.

Such nanostructured patterned samples were shown to guide and pattern liquid (FITC aqueous solution) or water drops with micrometer resolution. These results may have important

applications in several research fields, including microreactors,³⁴ microfluidics, and microchips.³⁵

Experimental Section

For sample preparation, the substrates, either glass slides or silicon wafers (1.5 cm × 1.5 cm), were first sonicated with ultrapure water (resistivity 18.2 MΩ·cm; ELGA) for 10 min and then treated with a 1:1:5 solution of 30% NH₃OH (J. T. Baker), 30% H₂O₂ (J. T. Baker), and water at 75 °C for 10 min, followed by treatment with a 1:1:5 solution of 30% HCl (J. T. Baker), 30% H₂O₂, and water at 75 °C for 10 min, with intermediate washing steps with deionized water after each treatment. Subsequently, the cleaned surfaces were exposed to 400 μL of 1% aminopropyltriethoxysilane (APTES, Sigma-Aldrich) aqueous solution for 5 min, washed with deionized water, and kept in vacuum overnight to remove the unbound APTES molecules. These samples were coated with thin films of silver of the desired thickness using a thermal evaporator and then exposed to HAuCl₄ (Sigma-Aldrich) aqueous solutions (the optimal reaction conditions were found to be 10⁻³ M HAuCl₄, 10 min of incubation at room temperature, see the text). For the fabrication of patterned flat/rough gold samples, cleaned APTES-modified substrates were first coated with a 50-nm-thick flat gold film and then different masks of resist layers (e.g., squares or stripes) were defined on them, allowing the selective deposition of a 50 nm silver film only into the exposed regions of the gold film. After the resist removal with acetone, these samples were incubated, for the SGDR process, with HAuCl₄ aqueous solutions, followed by extensive washing in deionized water and drying in a flow of nitrogen.

(34) Wang, Z.; Shang, H.; Lee, G. U. *Langmuir* **2006**, *22*, 6723–6726.

(35) Gau, H.; Herminghaus, S.; Lenz, P.; Lipowsky, R. *Science* **1999**, *283*, 46–49.

To fabricate the Si/Au patterns, a similar procedure was performed. After defining suitable resist masks on silicon wafers by optical lithography, samples were immersed in a 10⁻³ M HAuCl₄ aqueous solution with 1 M HF and 2 M NH₄F to facilitate the dissolution of SiO₂ (10 min of incubation time at room temperature), followed by washing in deionized water, lift-off in acetone, and drying in a flow of nitrogen. All of these substrates were characterized by optical microscopy, holographic microscopy (Lyncée Tec DHM 1000, transmission mode), AFM (Nanoscope IV MultiMode, Veeco Instruments), and SEM (Nova NanoSEM200, FEI).

The wettability properties of the various flat/nanorough substrates were assessed by measuring the contact angle of (bidistilled) water drops dispensed with a microsyringe onto the surfaces, with the sessile drop method. We used a CAM200-KSV instrument equipped with a digital camera to take magnified images of the microdroplets. The hydrophilic properties of Cys-modified rough gold stripes were investigated by depositing a 500 μL drop of an FITC aqueous solution (0.001%, Sigma-Aldrich) on the edge of the patterned rough/flat gold samples (the Cys functionalization was carried out before removal of the resist mask, leading to the selective surface modification of the rough gold stripes). Fluorescence measurements of the patterns were performed with a confocal microscope (Leica, TCS-SP5 AOB5).

Acknowledgment. We gratefully acknowledge S. Sabella, G. Vecchio, V. Brunetti, B. Sorce, and L. Martiradonna for useful discussions and help during experiments, and E. D'Amone and V. Fiorelli for expert technical assistance. This work was supported by the Italian Ministry of Research through the MIUR “FIRB” project (RBLA03ER38_001).